

Analytical and Monte Carlo Studies of the Interfacial Region in Semicrystalline Polymers with First- and Second-Order Intrachain Interactions

Ignacio Zúñiga,[†] Klein Rodrigues, and Wayne L. Mattice*

Institute of Polymer Science, The University of Akron, Akron, Ohio 44325

Received November 2, 1989; Revised Manuscript Received March 2, 1990

ABSTRACT: The partition function for the interfacial region of a semicrystalline polymer has been obtained in the frame of cubic lattice model. This is basically a reformulation of the lattice theory developed by Flory, Yoon, and Dill. Two independent contributions to the energy have been introduced to take into account the chain stiffness. Numerical results obtained by maximization of the partition function are satisfactory compared with those of other analytical models in the literature. The results are also compared with Monte Carlo simulations carried out by Mansfield and found to be in agreement only for small values of the bending energy. We have performed additional Monte Carlo simulations in order to explain the discrepancy for larger values of the bending energy, which arise from finite size effects.

I. Introduction

Several models have been proposed to describe the interphase in lamellar semicrystalline polymers. It is well established that the semicrystalline interphase is not sharp but instead extends for a certain distance in which a transition from the perfect order of the crystal to the disorder in the isotropic amorphous region occurs (for references to pioneering work see for instance ref 1). It is also clear that the order gradient requires that a substantial fraction of the chains emerging from a crystal reenter the same crystal.

A quantitative analysis of the chain conformation in the interphase was given by Mansfield² with Monte Carlo simulations in a cubic lattice. In the calculations, three independent energy contributions were included. The first one represents the so-called bending energy, i.e., the energy difference between a pair of collinear bonds and a pair of bonds at right angles. This is a way to model the stiffness of real chains in which a trans conformation has a smaller internal energy than a gauche conformation. The second energy contribution disfavors tight reversal conformations, which in a cubic lattice corresponds to two consecutive right angles in the same direction. The third contribution takes into account van der Waals interaction between chain segments. One of his conclusions is that, for completely flexible chains (in which the three above-mentioned energetic contributions are neglected), 72% of the stems emerging from the crystal reenter it by forming tight folds.

An analytical approach to the problem was done by Flory, Yoon, and Dill¹ (FYD). They approximated the partition function for the interphase in the frame of a cubic lattice theory. Two independent parameters were included in order to take into account the contributions to energy from both bending and tight reversal of the chains. Although their results are in qualitative agreement with Mansfield's conclusions, they found that for completely flexible chains only 42% of the chains are involved in tight-fold reentries.

The first attempt at solving the discrepancy between the two approaches was done by Marqusee and Dill.³ They calculated the entropy of the interphase by a mean-field lattice theory, extending a formalism derived by Helfand⁴

for a somewhat different problem. The first two degrees of approximation, up to two-bond conditional probability, were considered. In the case of completely flexible chains (their analysis is purely entropic) they showed that symmetry and normalization conditions on the two-segment conditional probabilities lead exactly to the constraints of the FYD model. However, they obtained that the fraction of tight-fold reentries is about 73%, which is in very good agreement with Monte Carlo² simulations. They suggested that the discrepancy mentioned above is due to an overcounting of the number of vertical bonds in the expression for the distribution function used in ref 1.

The approach was extended to account for chain stiffness by Marqusee.⁵ In the same mean-field approximation the internal energy of the interphase is calculated assuming only the contributions to the energy from bend junctions relative to straight ones. Then when the entropy expression derived in the previous papers^{3,4} is used, the Helmholtz free energy is minimized. The results were not compared with those of FYD, but the comparison with Mansfield's simulations showed that as the bending energy is increased there is no longer any quantitative agreement. For a value of the bending energy $\epsilon_b = kT$, Mansfield found that the percentage of tight folds reduces to 29%, but Marqusee obtained 52.2%.

More recently, Kumar and Yoon⁶ employed the same model to include the additional energy that the chain required to form a tight fold, but they did not include any bending energy. They made an extensive comparison with the results of FYD and Mansfield. The energy for a tight fold is denoted by η . They show that the content of tight folds deduced from their analytical treatment and from Mansfield's simulation is identical for $\eta \sim 6kT$. At smaller values of η , the simulations give a higher content of tight folds, and as η rises above $6kT$, the predictions from the two methods diverge, with simulations given the lower results.

In this paper we reformulate the FYD approach, i.e., instead of calculating the Helmholtz free energy from the entropy and the internal energy, we obtain directly the free energy from the partition function. In the approximation to the partition function we take into account a number of chain sequences that were not considered previously. We show that with this modification the results of the model are very close to those obtained in refs 3, 5, and 6.

[†] Present address: Departamento de Física Fundamental, Universidad Nacional de Educación a Distancia, Apartado 60141, 28080 Madrid, Spain.

In other words we prove that both approximate routes to the free energy are equivalent. Our results are also compared with Monte Carlo simulations,² and an explanation is given for the discrepancy between analytical methods and Monte Carlo simulations at large values of ϵ_b .

II. Model

In this paper we follow the notation used in ref 1, and we refer to that paper for most of the details. The model is based on the following assumptions. The system is represented by a cubic lattice where each site is occupied by a molecular segment. The segments of each chain are connected by linear bonds of equal length. The density is assumed to be uniform and the same as in the crystal because all the sites in the lattice are filled. In the crystalline region all bonds are parallel to a certain direction, which is normal to the plane of the anisotropic interphase. Layers of segments parallel to this plane are enumerated by an index i . In the isotropic amorphous region, which extends to positive values of i , we expect a random distribution of bonds among the six possible directions of the lattice. The number of layers from the crystal surface, $i = 0$, to the isotropic amorphous region defines the size of the anisotropic interphase. It is also assumed that the molecular chains are long enough so that there is a negligible number of chain ends.

A. Constraints. Let N_0 denote the number of sites per unit area in each layer and J_i the number density of bonds between layers $i - 1$ and i . We refer to those bonds as vertical bonds, and consequently we call the R_i bonds contained in layer i horizontal. A conservation condition follows directly from the above assumptions

$$2N_0 = J_i + J_{i+1} + 2R_i \quad (1)$$

It describes how the total number of bonds in layer i is distributed between vertical and horizontal bonds. In terms of the fractions $p_i = J_i/N_0$ and $q_i = R_i/N_0$, eq 1 reads

$$q_i = 1 - \frac{1}{2}(p_i + p_{i+1}) \quad (2)$$

If we define S_i^{++} as the number density of chains that reverse to layer $i + 1$, S_i^{--} as the number density of chains that reverse to layer $i - 1$, S_i^0 as the number density of chains that pass directly from layer $i - 1$ to $i + 1$, and S_i^\pm the number density of chains that pass from layer $i - 1$ to $i + 1$ but have at least one horizontal bond in layer i , the continuity of chains reduces to

$$J_i = 2S_i^{--} + S_i^\pm + S_i^0 \quad (3)$$

and

$$J_{i+1} = 2S_i^{++} + S_i^\pm + S_i^0 \quad (4)$$

Subtracting eq 3 from eq 4, we have

$$J_{i+1} - J_i = 2(S_i^{++} - S_i^{--}) \quad (5)$$

which can also be written as

$$p_{i+1} - p_i = 2(S_i^{++} - S_i^{--})/N_0 \quad (6)$$

Adding eqs 3 and 4, we obtain

$$J_{i+1} + J_i = 2S_i \quad (7)$$

where

$$S_i = S_i^{++} + S_i^{--} + S_i^\pm + S_i^0 \quad (8)$$

is the total number of chains in layer i . Note that the total number of chains that pass through from layer $i - 1$ to layer

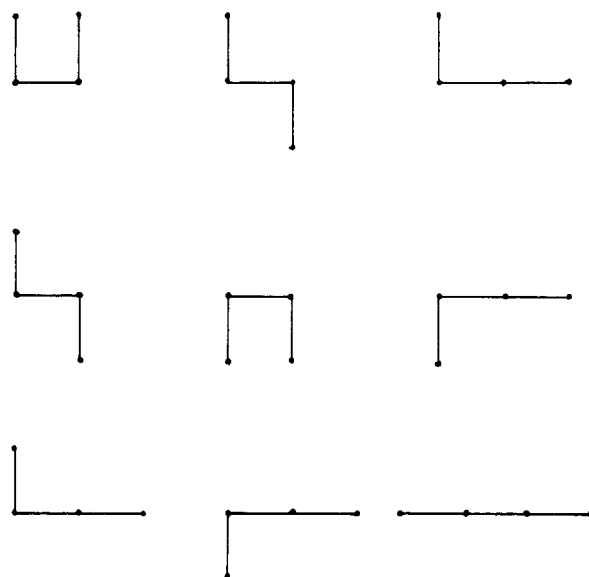


Figure 1. Conformations of three bonds in the same 3×3 array as the elements in the matrix of eq 10.

$i + 1$ includes both the number S_i^\pm of sequences with at least one horizontal bond and the number S_i^0 of sequences with two collinear vertical bonds. The latter kind of sequence was not considered by Flory, Yoon, and Dill.¹

Inserting eq 1 into eq 7, we obtain

$$N_0 = S_i + R_i \quad (9)$$

B. Statistical Distribution of Chain Sequences in the Interphase. Before we proceed, some more approximations have to be made. We assume the partition function for the interphase to be the product of the partition function for each layer. We also assume that in each site the orientation of a particular bond only depends on the position of the previous bond in the chain. In order to take into account the energy for tight reversal, we consider as chain units all possible three-bond sequences, with the exception of those S_i^0 two-bond sequences corresponding to chains that pass directly from layer $i - 1$ to $i + 1$.

If we call u_{i+} , u_{i-} , and u_{i0} the weighting factors for junctions at the end of a horizontal bond with an upward vertical bond, a downward vertical bond, and a horizontal bond, respectively, the a priori probabilities of occurrences of the possible three-bond sequences can be represented by the matrix (see Figure 1)

$$C_i = \begin{pmatrix} hu_+^2 & u_+u_- & u_+u_0 \\ u_-u_+ & hu_-^2 & u_-u_0 \\ u_0u_+ & u_0u_- & u_0^2 \end{pmatrix}_i \quad (10)$$

where

$$C_i^{-1} = 1 - (1 - h_i)(u_{i+}^2 + u_{i-}^2) \quad (11)$$

is the normalization factor when $u_+ + u_- + u_0 = 1$, and h_i is a parameter to modify the incidences of chain tight reversals.

One can now obtain expressions for all the stochastic variables that characterize the structure of the interphase. Furthermore, all those variables can be defined as functions of u_{i+} , u_{i-} , u_{i0} , and h_i . In particular, the number of several kinds of chains that have at least one horizontal bond in layer i is

$$S_i^{--} = R_i C_i u_{i-}^2 (u_{i+} + u_{i-})^{-1} [1 - (1 - h_i)(u_{i+} + u_{i-})] \quad (12)$$

$$S_i^{++} = R_i C_i u_{i+}^2 (u_{i+} + u_{i-})^{-1} [1 - (1 - h_i)(u_{i+} + u_{i-})] \quad (13)$$

and

$$S_i^{\pm} = R_i C_i u_{i-} u_{i+} (u_{i+} + u_{i-})^{-1} \quad (14)$$

therefore the total number of chains that have one or more horizontal bonds is

$$S_i^{++} + S_i^{--} + S_i^{\pm} = R_i (1 - C_i u_{i0}) \quad (15)$$

cf. eqs 10–19 in ref 1. Inserting the above expression and eq 8 into eq 9, we obtain that the number of chains passing directly from layer $i - 1$ to $i + 1$ is

$$S_i^0 = N_0 - R_i (2 - C_i u_{i0}) \quad (16)$$

There are nine possible sequences with at least one horizontal bond given by eq 10. For simplicity they can be arranged in some groups. FYD considered five groups of sequences: first three groups f_{i+} , f_{i-} , and f_{i0} , obtained by summing the rows of the matrix in eq 10, and two more groups that correspond to positive F_{i++} and negative F_{i--} tight reversals. The corresponding a priori incidences for each group are

$$\begin{aligned} f_{i+} &= C_i u_{i+} [1 - (1 - h_i) u_{i+}] \\ f_{i-} &= C_i u_{i-} [1 - (1 - h_i) u_{i-}] \\ f_{i0} &= C_i u_{i0} \\ F_{i++} &= C_i h_i u_{i+}^2 \\ F_{i--} &= C_i h_i u_{i-}^2 \end{aligned} \quad (17)$$

This choice is arbitrary. We have also tried another way of arranging the sequences that will be described later on.

C. Statistical Distribution of Chain Sequences in the Amorphous Region. In each layer the probability of having n_i incidences of a particular kind of sequence is ν^{n_i} , where ν is the a priori statistical weight of that sequence. Therefore, it will be necessary to introduce a priori statistical weights that complement the stochastic variables. This can be done by repetition of the above procedure but now in the amorphous region. Let τ values denote the statistical weight for a bend connection relative to 1 for a collinear connection. Therefore, the relative probability of a particular bend connection of two bonds in a cubic lattice is $\lambda = \tau / (1 + 4\tau)$ and the relative probability of a collinear connection is $\delta = 1 / (1 + 4\tau)$. The conditional probability of a connection at the end of a horizontal bond to another horizontal bond is

$$\sigma = (1 + 2\tau) / (1 + 4\tau)$$

It is clear that the conditional probability of a connection at the end of a horizontal bond to a vertical upward bond or to a vertical downward bond is

$$\lambda = (1 - \sigma) / 2$$

In a cubic lattice the a priori statistical weight for a vertical bond is $1/3$ and consequently the a priori probability for a site with two collinear vertical bonds is $\delta/3$. (For a completely flexible chain $\tau = 1$, $\sigma = 3/5$, and $\delta = 1/5$.) We also include a parameter, η , for the a priori weight for adjacent return.

Straightforward substitutions of u_{i+} , u_{i-} , u_{i0} , and h_i by λ , λ , σ , and η , respectively, in the equations for the a priori incidences give the a priori probabilities of various sequences. The a priori probabilities of the various

adjacent returns are

$$\Phi_{++} = \Phi_{--} = \Gamma \eta \lambda^2 \quad (18)$$

and the corresponding probabilities for f_{i+} , f_{i-} , and f_{i0} are

$$\begin{aligned} \phi_+ &= \phi_- = \Gamma \lambda [1 - \lambda(1 - \eta)] \\ \phi_0 &= \Gamma \sigma \end{aligned} \quad (19)$$

where

$$\Gamma^{-1} = \left[1 - \frac{1}{2}(1 - \eta)(1 - \sigma)^2 \right]$$

is the normalization constant equivalent to C_i .

D. Partition Function. The exact partition function depends on the allocation of S_i chains in layer i . However, we approximate the partition function so that we only calculate the probability of different sequences of three bonds. We have tried several approximations. We first discuss the closest one to that used by FYD.

1. First Approximation. Let us rewrite eq 16 as

$$N_0 = S_i^0 + R_i^* \quad (20)$$

where

$$R_i^* = R_i (2 - C_i u_{i0}) \quad (21)$$

We consider the partition function as the product of two factors. The first factor, Ω_{Ii} , depends on the allocation of S_i^0 sites with two collinear vertical bonds and R_i^* sites with at least one horizontal bond (cf. eq 20). Note that $R_i C_i u_{i0}$ is the correction due to the sequences with more than one horizontal bond.

The a priori probability of a site with two vertical bonds is $\delta/3$ and the a priori probability of one of the other sequences, i.e., with at least one horizontal bond is $1 - \delta/3$. Therefore the first factor can be written as

$$\Omega_{Ii} = \left(\frac{\delta}{3} \right)^{S_i^0} \left(1 - \frac{\delta}{3} \right)^{R_i^*} \binom{N_0}{S_i^0} \quad (22)$$

For the second factor, Ω_{IIi} , which depends on the distribution of R_i horizontal bonds among the possible sequences, we use the expression given by eq 28 in ref 1. In order to compare with the approximation introduced by FYD, note that their expression for the first factor was obtained by the allocation of N_0 bonds between J_i vertical and R_i horizontal bonds (see eq 1). But the vertical bonds are also counted in the sequences considered in the second factor. This overcounting of vertical bonds led to an underestimation for the partition function as was pointed out by Marqusee and Dill.³ It will be shown later that both models give similar results for high values of η . This is due to the fact that in such a case there is a wide region of the interphase where most of the bonds are vertical so that $J_i \approx S_i^0$ and consequently $R_i^* \approx R_i$. Under those approximations eq 22 reduces to

$$\Omega_{Ii} = \left(\frac{1}{3} \right)^{J_i} \left(\frac{2}{3} \right)^{R_i} \binom{N_0}{R_i} \quad (23)$$

which is the equation employed by FYD.

2. Second Approximation. In this approximation we use eq 22, but the second factor in the partition function is modified. The difference with the first approximation is how to form the groups of sequences. We now choose the following groups: F_{i++} (element 1,1 of the matrix in eq 10) and F_{i--} (element 2,2) as before and then the number of sequences corresponding to chains that pass from layer $i - 1$ to layer $i + 1$ and have only one horizontal bond

elements 1,2 and 2,1)

$$S_{i;1}^{\pm} = 2R_i C_i u_{i+} u_{i-}$$

and their a priori probability

$$\Sigma_1^{\pm} = 2\Gamma\lambda^2$$

The number of sequences not included in the above three groups with a vertical upward bond (elements 1,3 and 3,1) is

$$f_{i+}' = 2R_i C_i u_{i0} u_{i+}$$

and the corresponding probability is

$$\phi_+' = 2\Gamma\lambda\sigma$$

The number of sequences not included in the above groups with one vertical downward bond (elements 2,3 and 3,2) is

$$f_{i-}' = 2R_i C_i u_{i0} u_{i-}$$

and the corresponding probability is

$$\phi_-' = 2\Gamma\lambda\sigma$$

Finally the number of sequences with three horizontal bonds (element 3,3) is

$$f_{i0}' = C_i R_i u_{i0}^2$$

and its probability is

$$\phi_0' = \Gamma\sigma^2$$

The reason to choose this way of group sequences is that now all the sequences in each group have the same a priori probability, making it more instructive to the partition function. The second factor in the partition function now reads

$$\Omega_{11i} = \frac{R_i!}{S_{i;1}^{\pm} F_{i+}' F_{i-}' f_{i0}'} \times \left[(\Sigma_1^{\pm})^{S_1^{\pm}} (\Phi_{++})^{F_{i+}'} (\Phi_{--})^{F_{i-}'} (\phi_+)^{f_{i+}'} (\phi_-)^{f_{i-}'} (\phi_0')^{f_{i0}'} \right]^{R_i} \quad (24)$$

3. Third Approximation. In both previous approximations we have assumed that all junctions of two horizontal bonds are of the same sort. To properly include bending and tight-folding energies, we should differentiate between straight junctions and bend junctions. In this case instead of one horizontal conditional probability, u_0 , one has to consider the conditional probability, u_s , of having at the end of a horizontal bond another collinear horizontal bond and the corresponding probability, u_b , for a bend connection between two horizontal bonds. This extra conditional probability was also considered by both Marqusee⁵ and Kumar and Yoon.⁶ On the basis of the fact that there are no imposed boundary conditions on the horizontal directions, Marqusee⁵ showed that u_s and u_b simply obey the Boltzmann relation.

We are not going to give all the details because the procedure is almost exactly the one we have already described.

In this approximation the possible sequences in each layer are

$$C_i = \begin{pmatrix} hu_+^2 & u_+u_- & u_+u_s & 2u_+u_b \\ u_-u_+ & hu_-^2 & u_-u_s & 2u_-u_b \\ u_su_+ & u_su_- & u_s^2 & 2u_su_b \\ 2u_bu_+ & 2u_bu_- & 2u_bu_s & 2u_b^2(h+1) \end{pmatrix} \quad (25)$$

where

$$C_i^{-1} = 1 - (1 - h_i)(u_{i+}^2 + u_{i-}^2 + 2u_{ib}^2) \quad (26)$$

and

$$u_{i+} + u_{i-} + u_{is} + 2u_{ib} = 1$$

In the amorphous region we have $u_{i+} = u_{i-} = \lambda$, $u_{is} = \delta$, $u_{ib} = \lambda$. The various groups of sequences and their respective a priori probabilities are

$$\begin{aligned} F_i^{++} &= C_i h_i u_{i+}^2 & \Phi_{++} &= \Gamma\eta\lambda^2 \\ F_i^{--} &= C_i h_i u_{i-}^2 & \Phi_{--} &= \Gamma\eta\lambda^2 \\ F_i^b &= 2C_i h_i u_b^2 & \Phi_b &= 2\Gamma\eta\lambda^2 \\ S_{i;1}^{\pm} &= 2C_i u_{i+} u_{i-} & \Sigma_1^{\pm} &= 2\Gamma\lambda^2 \\ f_{i+}^s &= 2C_i u_{is} u_{i+} & \phi_+^s &= 2\Gamma\lambda\delta \\ f_{i-}^s &= 2C_i u_{is} u_{i-} & \phi_-^s &= 2\Gamma\lambda\delta \\ f_{i+}^b &= 4C_i u_{ib} u_{i+} & \phi_+^b &= 4\Gamma\lambda^2 \\ f_{i-}^b &= 4C_i u_{ib} u_{i-} & \phi_-^b &= 4\Gamma\lambda^2 \\ f_{i0}^s &= C_i u_{is}^2 & \phi_0^s &= \Gamma\delta^2 \\ f_{i0}^b &= 4C_i u_{ib} u_{is} & \phi_0^b &= 4\Gamma\delta\lambda \\ f_{i0}^{bb} &= 2C_i u_{ib}^2 & \phi_0^{bb} &= 2\Gamma\lambda^2 \end{aligned} \quad (27)$$

where

$$\Gamma = 1 - 4(1 - \eta)\lambda^2 \quad (28)$$

The number density of negative reversals containing l horizontal bonds in layer i is

$$\begin{aligned} S_{i;l}^{--} &= R_i C_i h_i u_{i-}^2 & l &= 1 \\ S_{i;l}^{--} &= R_i C_i (u_{is} + 2u_{ib}) u_{i-}^2 & l &= 2 \end{aligned} \quad (29)$$

$$S_{i;l}^{--} = R_i C_i [(u_{is} + 2u_{ib})^2 + 2u_{ib}^2(h_i - 1)] u_{i-}^2 \quad l = 3$$

summation over l gives

$$S_i^{--} = C_i R_i u_{i-}^2 [h_i + u_{i0}(1 + u_{i0}) + 2u_{ib}^2(h_i - 1)] \quad (30)$$

where $u_0 = u_s + 2u_b$ and we have neglected terms smaller than u_0^2 . Similarly

$$S_i^{++} = C_i R_i u_{i+}^2 [h_i + u_{i0}(1 + u_{i0}) + 2u_{ib}^2(h_i - 1)] \quad (31)$$

$$S_i^{\pm} = 2C_i R_i u_{i+} u_{i-} [u_{i0}(1 + u_{i0}) + 2u_{ib}^2(h_i - 1)] \quad (32)$$

The total number of chains in layer i with one, two, or three horizontal bonds is

$$S_i - S_i^0 = S_i^{++} + S_i^{--} + S_i^{\pm} = C_i R_i \{ (u_{i+}^2 + u_{i-}^2) h_i + (u_{i+} + u_{i-})^2 [u_{i0}(1 + u_{i0}) + 2u_{ib}^2(h_i - 1)] \} \quad (33)$$

The above equation is the equivalent to eq 15 in this approximation. Note that in the two previous approximations the summation over l has been extended to infinity, but in this case it was only extended up to three horizontal bonds.

E. Computational Procedure. The partition function for the interphase is maximized subject to the following boundary conditions at the first layer¹

$$u_{1+} = 0, \quad u_{1-} = 1, \quad u_{10} = 0 \quad (34)$$

The boundary conditions reflect the fact that, in the first layer of the interphase, all the horizontal bonds have to

Table I
Fraction of Tight Folds vs Bending Energy

<i>b</i>	Mansfield	Marqusee	FYD ^a	approx 1	approx 2	approx 3
0	0.720	0.733	0.420	0.746	0.733	0.772
1	0.298	0.522	0.380	0.509	0.535	0.569
2		0.297	0.333	0.288	0.349	0.376

^a The data corresponding to this column are from our own calculations using their approximation.

reenter the crystallite; otherwise, there would be sites with more than two bonds. On the other hand $p_1 = 1$ because the crystal is assumed perfect. Therefore, given q_1 , u_{i+} , u_{i-} , and h_i , we can determine the partition function. The values of the stochastic variables that make the partition function a maximum describe the interphase at equilibrium. The maximization was carried out numerically by using a routine based on Powell's method.⁷ We refer to ref 1 for more details on the computational procedure.

III. Results and Discussion

In spite of a variety of methods used in the literature and the quantitative discrepancy among some of them, most of papers give the same qualitative picture of the structure of the interphase. We therefore refer to refs 1–3 and 6 for a discussion on how the properties of the interphase may change with bending and tight reverse energies. In this section we concentrate on showing our results and compare them with others in the literature.

A. Effect of Bending Energy. In Table I are listed our results for the fraction of tight folds for three values of bending energy. They are compared with previous results in the literature. In order to make the comparison easier, we list the parameter $-b$ used by Mansfield,² which, when there is no van der Waals interaction, corresponds to $\epsilon_b = -b$ used in ref 5 and to $\tau = \exp(b)$ employed in ref 1 and in this paper. All the values given in this paper for the FYD model have been computed by us by using exactly the model described in ref 1.

The first thing to remark is that the results with our approximations 1–3 and Marqusee's results are in fairly good agreement, which suggests that the lattice model is not very sensitive to mathematical refinements. This characteristic of the lattice model was pointed out in a rather different context by Flory.⁸ We also list the results obtained with the FYD model to show how as the stiffness of the chain increases their results are in better agreement with our models.

There is also agreement with the results obtained by Monte Carlo simulations² when $b = 0$; however, this is in contrast with the case $b = 1$. In order to investigate the origin of this discrepancy, we have carried out some Monte Carlo simulations for several values of the parameter b , using the same code describe in ref 9. In the simulation there are 30 layers in the cubic lattice; Mansfield's lattice had 31 layers.

The results are plotted in Figures 2 and 3. In Figure 2 we plot the fractions of tight folds versus b obtained by both Monte Carlo simulation and by our first analytical model. For values of b smaller than 0.7 both Monte Carlo and the analytical results follow the same trend. However, for values of b larger than 0.7 we observe a dramatic drop of the tight-fold fraction obtained with Monte Carlo. This is in contrast with the results from the analytical model that show the same linear dependence on b .

The parameter $\gamma = 2n_z/(n_x + n_y)$, where n_x , n_y , and n_z are the fractions of two collinear bonds along the x , y , and z axes, respectively, takes the value 1 in the amorphous

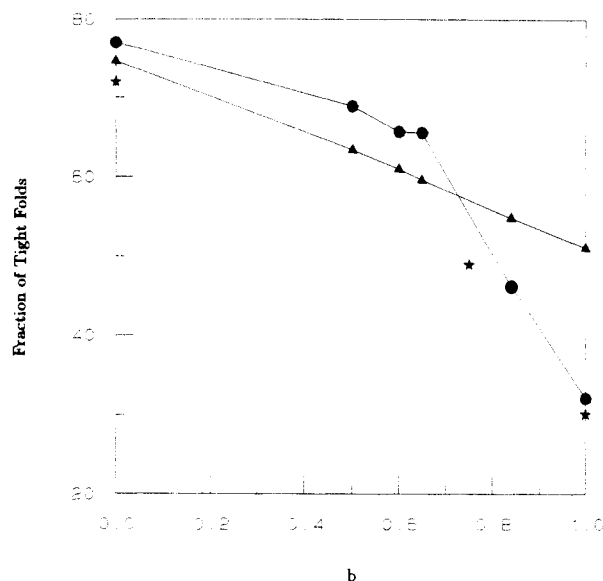


Figure 2. Tight folds vs the weighting factor for a bend for the first approximations described in the present work (triangles) and Monte Carlo simulations by Mansfield (stars) and from the present work (circles).

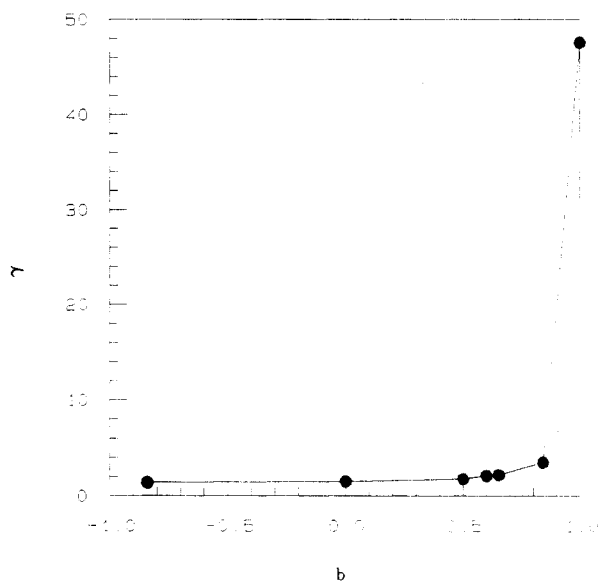


Figure 3. Dependence of $\gamma = 2n_z/(n_x + n_y)$ on b in Monte Carlo simulations on a cubic lattice with 30 layers.

region and is infinity in the crystalline region where all the bonds are along the z axis. In Figure 3 we plot the value of γ in the middle of the lattice as a function of b . We observe that for values of $b > 0.8$ the middle layer of the lattice is not amorphous. Therefore, the sharp drop in the fraction of tight folds at large b in the Monte Carlo simulations in Figure 2 could be due to the fact that the lattice used is not large enough. Alternatively stated, the analytical method assumed that the interfacial region is bounded on one side by the crystal and on the other side by an amorphous region. For lattices of the sizes used in the Monte Carlo simulations, this state of affairs is obtained at $b < 0.8$ but not at $b > 0.8$. The Monte Carlo simulations should not be expected to agree with the analytical method at $b > 0.8$ because the system is different. At $b > 0.8$, the Monte Carlo method examines a partially disordered region between two crystal faces that are so close together that no part of the system can avoid the influence of the crystal. Presumably the Monte Carlo simulations would agree with the analytical results over the entire range covered in Figure

Table II
Fraction of Vertical Bonds

<i>b</i>	layer	approx 1	approx 2	approx 3	Marqusee
0	1	1.0	1.0	1.0	1.0
0	2	0.252	0.267	0.228	0.268
0	3	0.350	0.344	0.244	0.340
0	4	0.332	0.332	0.243	0.332
0	5	0.334	0.334	0.243	0.334
1	2	1.0	1.0	1.0	1.0
1	2	0.49	0.466	0.431	0.478
1	3	0.325	0.338	0.278	0.358
1	4	0.334	0.334	0.253	0.338
1	5	0.333	0.333	0.248	0.334
1	6	0.333	0.333	0.247	
2	1	1.0	1.0	1.0	1.0
2	2	0.712	0.651	0.624	0.704
2	3	0.370	0.415	0.345	0.522
2	4	0.339	0.353	0.317	0.428
2	5	0.334	0.338	0.301	0.380
2	6	0.333	0.335	0.293	0.340

Table III
Order Parameter

<i>b</i>	layer	Marqusee	FYD	approx 1	approx 2	approx 3
0	1	0.451	0.685	0.441	0.450	0.421
0	2	-0.045	0.190	-0.053	-0.042	-0.146
0	3	0.005	0.005	0.006	0.007	-0.135
0	4	-0.001	0.000	-0.001	-0.001	-0.135
1	1	0.608	0.715	0.618	0.599	0.573
1	2	0.127	0.234	0.112	0.103	0.031
1	3	0.022	0.021	-0.006	0.004	-0.102
1	4	0.004	0.002	0	0	-0.124
1	5	0	0	0	0	-0.124
2	1	0.772	0.751	0.784	0.739	0.718
2	2	0.419	0.297	0.312	0.300	0.227
2	3	0.213	0.060	0.032	0.076	-0.004
2	4	0.107	0.016	0.004	0.019	-0.037
2	5	0.053	0.004	0.001	0.005	-0.037
2	6	0.026	0.001	0	0.001	-0.037

1 if they were performed in a much larger box, such that the middle of the box is amorphous. This statement must remain as a conjecture because of the practical problems associated with a large increase in the size of the box in the simulations.

In Table II are listed the weighting factors for the three approximations. One can see how u_s and u_b obey the Boltzmann relation. A comparison with the results of Marqusee shows quite good agreement for the first and second approximations. However, for the third approximation we find that in the interface u_{i+} is smaller and u_{i-} is larger than the corresponding values obtained by Marqusee.⁵ As a consequence we obtain an excess of horizontal bonds. This can be seen in Table III where the order parameter is listed for our three approximations for several values of the bending energy. For approximations 1 and 2, this means that the interphase region is shorter, but for approximation 3 we observe that the order parameter, instead of going to zero, tends to a negative asymptotic value. This effect is more noticeable as the bending energy is increased. There are basically two differences in the third approximation. In the first difference we introduce an extra probability for horizontal junctions so that we can now distinguish between two collinear horizontal bonds and two horizontal bonds at right angles. The second difference, which is a consequence of the first one is that now we have truncated the summation of chains in each layer to sequences of three horizontal bonds (see eqs 30–32) while in approximations 1 and 2 the summation was extended to infinity. Somehow what we gain with the refinement is lost in the approximated sum.

Table IV
Fraction of Tight Folds vs Folding Energy

<i>c</i>	Mansfield	KY	FYD ^a	approx 1	approx 2	approx 3
0	0.720	0.733	0.42	0.746	0.733	0.772
2	0.46	0.54	0.246	0.544	0.565	0.638
5	0.319	0.36	0.146	0.305	0.369	0.349
10	0.287	0.2	0.129	0.213	0.211	0.225

^a The data corresponding to this column are from our own calculations using their approximation.

Table V
Order Parameter

<i>c</i>	layer	KY	FYD	approx 1	approx 2	approx 3
0	1	0.45	0.68	0.44	0.45	0.42
0	2	-0.05	0.19	-0.05	-0.04	-0.15
0	3	0	0	0	0.01	-0.13
2	1	0.59	0.82	0.59	0.57	0.522
2	2	0.09	0.33	0.06	0.04	-0.090
2	3	0	0.02	-0.05	-0.04	-0.17
2	4	0	0	-0.03	-0.03	-0.17
10	1	0.85	0.90	0.84	0.84	0.83
10	2	0.53	0.61	0.37	0.40	0.33
10	3	0.28	0.22	0.00	-0.03	-0.08
10	4	0.1	0.01	-0.04	-0.04	-0.17
10	5	0.02	0	-0.04	-0.04	-0.17

Table VI
Average Length of Horizontal Sequences vs Tight-Fold Energy

<i>c</i>	KY	FYD	approx 1	approx 2	approx 3
0	2.47	2.5	2.51	2.50	2.50
2	2.96	3.3	3.29	3.30	3.29
5	3.83		3.49	3.49	3.49
10	5.29	3.5	3.50	3.50	3.50

B. Effect of Tight-Fold Energy. In this section we make a comparison between the results from our various approximations and previous results found in the literature in the case that the only contribution to the energy is from a tight fold. This is not a realistic situation, but it allows us to compare the effect of this contribution to the energy that was not considered by Marqusee.⁵ Tables IV–VI we use again Mansfield's notation for the parameter c describing this energy. This parameter corresponds to E_η used in ref 6 and to $\eta = \exp(-c)$ employed in ref 1 and in this paper.

The fraction of tight folds versus energy is shown in Table IV. Not surprisingly, our results agree with those of Kumar and Yoon,⁶ as their model is basically the same as the one used by Marqusee and Dill.³ They also agree with Monte Carlo simulations at least for the range of values of the energy with physical meaning for polyethylene.

Kumar and Yoon⁶ carried out some computations for values of c up to 20 at which the fraction of tight folds approaches zero. We have also carried out some calculations for such high values of c , even though they are unphysical for polyethylene. We found an increasing difficulty for the algorithm to find the minimum. Our results show a slower decrease in the fraction of tight folds, 11% for $c = 20$. In Table VI we write the average length of horizontal chain sequences. For small values of c all the models are in good agreement. For higher values of the parameter c we observe that the average length tends to an asymptotic limit of about 3.5. This is the expected behavior for the following reason: Increasing the value of c produces an attrition of tight reversals, which would increase the average length of horizontal chain sequences. However, further increments of c as the number of tight reversals vanishes should not affect the properties of the

interphase. This is in contrast with Kumar and Yoon,⁶ where the average length of horizontal sequences seems to grow without bound. As the authors pointed out, this unphysical result may be due to their assumption of having a tight-fold energy without including an independent bending energy.

In Table V are listed the values of the order parameter for three values of c . Note that we observe again that the order parameter does not go to zero, but it tends to a negative value. As the tight-fold energy is increased, this effect is shown by the three approximations.

C. Conclusions. Our results have also been compared with Monte Carlo simulations.² We have found that there is no agreement when bending energy is larger than 0.8. We believe that this disagreement is due to the fact that the lattice used in the Monte Carlo simulations is not large enough to provide two independent interphases at the top and bottom of the lattice for high values of the bending energy.

From a comparison of the results obtained from our three approximations we found that the lattice model does not necessarily give better results with mathematical refinements. The second model is the simplest one and gives in most of the cases the most accurate results. We

will therefore choose the second model in subsequent work where we study the effect of branches in the interface.

Acknowledgment. This research was supported by the National Science Foundation (Grant DMR-8706166), the donors of the Petroleum Research Fund, administered by the American Chemical Society, and by a NATO fellowship (I.Z.).

References and Notes

- (1) Flory, P. J.; Yoon, D. Y.; Dill, K. A. *Macromolecules* **1984**, *17*, 862-868.
- (2) Mansfield, M. L. *Macromolecules* **1983**, *16*, 914-920.
- (3) Marqusee, J. A.; Dill, K. A. *Macromolecules* **1986**, *19*, 2420-2426.
- (4) Helfand, E. *Macromolecules* **1976**, *9*, 307-310.
- (5) Marqusee, J. A. *Macromolecules* **1989**, *22*, 472-476.
- (6) Kumar, S. K.; Yoon, D. Y. *Macromolecules* **1989**, *22*, 3458-3465.
- (7) Subroutine POWELL: Press, W. H.; Flannery, B. P.; Teukolsky, S. A.; Vetterling, W. T. *Numerical Recipes*; Cambridge University Press: Cambridge, U.K., 1986.
- (8) Flory, P. J. *Principles of Polymer Chemistry*; Cornell University Press: Ithaca, NY, 1953; footnote on p 500 and p 504.
- (9) Mathur, S. C.; Rodrigues, K.; Mattice, W. L. *Macromolecules* **1989**, *22*, 2781-2785.

γ -Isotactic Polypropylene. A Structure with Nonparallel Chain Axes

S. V. Meille,^{*,†} S. Brückner,[‡] and W. Porzio[§]

Dipartimento di Chimica del Politecnico di Milano, Piazza Leonardo da Vinci, 32, 20133 Milano, Italy, Istituto di Chimica della Università di Udine, Viale Ungheria, 43, 33100 Udine, Italy, and Istituto di Chimica delle Macromolecole del CNR, Via E. Bassini, 15, 20133 Milano, Italy

Received October 10, 1989; Revised Manuscript Received February 12, 1990

ABSTRACT: The crystal structure of the γ form of isotactic polypropylene (γ -iPP) is refined with the Rietveld method on X-ray diffraction data collected at low (-120°C) temperature. The analysis, leading to the proposal of the totally novel crystal architecture with nonparallel chain axes, is discussed in detail, and the reliability of the proposed structure is assessed, also with reference to alternative models. While the overall structure is best represented in terms of the statistical copresence of anticlinal isochiral helices at each crystallographic position, as implied by space group $Fddd$, local packing modes which cannot retain this feature are satisfactorily described in terms of space groups $F2dd$ or $Fd2d$. Some relevant implications of the γ -isotactic polypropylene crystal structure on the crystalline morphology of this polymer are presented, while issues concerning the development of this novel architecture remain largely open to future contributions.

1. Introduction

The γ modification of crystalline isotactic polypropylene (γ -iPP) has attracted much attention over the years although interest in this polymorph for immediate applications has been modest, as it is obtained usually only in traces under normal crystallization conditions with commercial homopolymers. The appearance of the γ phase is favored by a molecular feature such as shortness of polymer chains¹ or, for long chains, by a physical variable such as high pressure.² An interesting paper by Turner-

Jones describes also the influence that small amounts of comonomer units (4-10% ethylene or 1-butene) exert in promoting γ rather than α crystallinity in melt-crystallized copolymers,³ which have indeed industrial importance.

High percentages of γ crystallinity are also obtained⁴ with iPP synthesized with new homogeneous catalytic systems⁵ for which future applications may be envisaged.

Crystallization in the γ phase has been related^{6,7} to the reduced importance of chain folding, and investigations on the differences between the α and γ phases may contribute to clarification of this issue at a molecular level. A study on the relationships between chain folding and crystal structure was carried out for α -iPP, revealing the existence of a number of "selection rules" for neighboring

^{*} Dipartimento di Chimica del Politecnico di Milano.

[†] Istituto di Chimica della Università di Udine.

[§] Istituto di Chimica delle Macromolecole del CNR.